BJRS

BRAZILIAN JOURNAL
OF
RADIATION SCIENCES
10-03A (2022) 01-15

SBPR
Sociedade Brasileira de Proteção Radiológica

Encapsulated OSB Energy Absorption Potential: A preliminary analysis

Carvalho[a] D.S.M., Mattar Neto[a] M.

[a] *Nuclear and Energy Research Institute IPEN-CNEN, 05508-000, São Paulo, São Paulo, Brazil*

dancarvalho@usp.br and mmattar@ipen.br

ABSTRACT

The transport of radioactive substances is, in many ways, necessary in the context of the nuclear fuel cycle that aims to generate energy or radioisotopes. In the event of a possible accident, the shock-absorbing parts reduce the mechanical stresses on the other components of the transport packaging, since a large part of the kinetic energy is absorbed by the shock absorber. To standardize the design of the research reactor spent fuel assembly transport devices by numerical analysis, a set of dynamic simulations of a benchmark was conducted to representatively capture the phenomena found in the drop tests used in project qualifications. This study aims to present a comparison of different ways of applying wood and wood composites as a useful and accessible impact-absorbing material. The necessary numerical modelling characteristics are validated and the phenomena present in non-isotropic materials are discussed. This study demonstrates the application of material models where energy absorption is the main structural function. In this case, the orientation of the wood fibers became sensitive with an approximate difference of 10% more in the impact absorption potential, without considerable variation in the duration interval of the maximum deceleration.

Keywords: **Shock absorbers, Wood, Cellular solids, Finite elements method, Ls-dyna.**

ISSN: 2319-0612
DOI: https://doi.org/10.15392/2319-0612.2022.1874
Submitted: 2022-01-27
Accepted: 2022-09-29

1. INTRODUCTION

The transport of radioactive substances is, in many ways, necessary in the context of the nuclear fuel cycle that aims to generate energy or radioisotopes. The research reactors spent fuel packages used for transporting and storing are equipped with bolted or welded locking systems and are mainly, supplied with shock-absorbing parts. In the event of a possible accident, the shock-absorbing parts reduce the mechanical stresses on the other components of the transport packaging, since a large part of the kinetic energy is absorbed by them, which, compared to the container and the impact body, is more resilient [1].

The container must provide shielding to protect workers, the public, and the environment from the effects of radiation, to prevent an unwanted chain reaction, heat damage, and also protect against dispersion of the contents. To standardize the design of this type of transportation devices by numerical analysis, a set of dynamic simulations was conducted to representatively capture the phenomena found in the drop tests used in project qualification [1].

This study aims to present a comparison of different ways of applying wood and wood composites as a useful and accessible impact-absorbing material. The necessary numerical modelling characteristics are validated, and the phenomena present in non-isotropic materials are discussed in the numerical simulations of a drop test benchmark described in [2].

2. KNOWN SO FAR

To start interpreting the phenomena and characteristics of wood and wood composites, it is first necessary to define what cellular solids are. They are composed of an interconnected network of supports or solid shells that forms the edges and faces of cells. Typically, as is in one of three different formations, as shown in Fig. 1. The simplest, Fig.1(a), is formed by a two-dimensional array of polygons that groups together to fill a flat area with hexagonal cell materials such as honeycombs. Most commonly, cells are made up of polyhedral that cluster in three dimensions to fill space; also called three-dimensional cellular materials foams. If the solid from which the foam is made is contained only at the edges of the cells (so that the cells connect through open faces), the foam is said to be an open-cell, Fig. 1(b). If the faces are also solid, such that each cell is sealed off from its neighbors, it is said to be a closed-cell, Fig. 1(c); and, of course, some foams are partially open and partially closed [3].

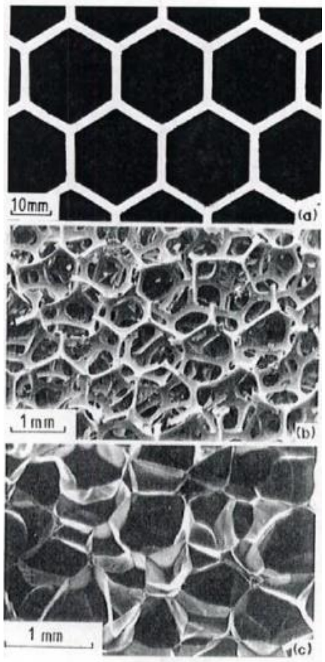

Figure 1: *Main cellular solid formations - 1(a) polygons; 1(b) solid faces; 1(c) open and closed foams*
Source: [3]

The control of the different properties of wood and wood composites is such that it is hard to establish a material model and the respective constitutive equations to cover each variation, species, formation, characteristic or origin. However, it is possible to propose a progression in adding different complexities allowing studying their effects at each step.

Fig. 2 tries to summarize this procedure, so that the most recommended step is chosen for a given application, considering the properties of the Material (elasticity, viscoelasticity, plasticity, humidity, temperature), the Anisotropy (longitudinal, radial, and tangential), the Structure (Polar Orthotropic, Grain Direction, Density, Cell Structure, Knots) and Heterogeneity (Earlywood, Latewood, Fibers, Ray Cells, Heartwood, Knots).

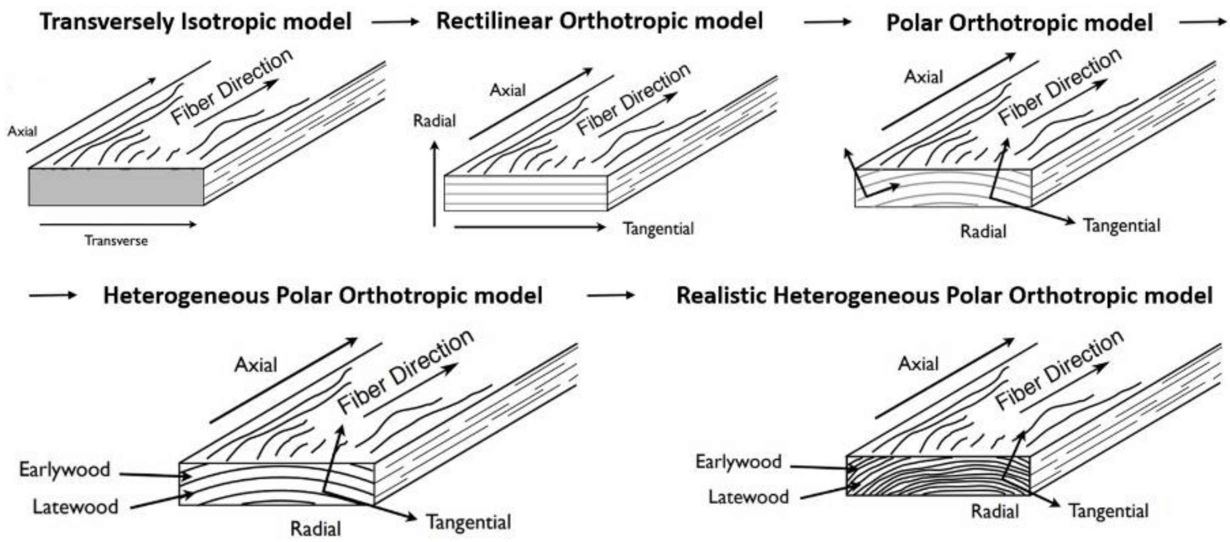

Figure 2: *Mapping Wood Complexities.*
Source: modified from [4]

The most direct wood factors to be considered in numerical modeling are: (i) Fiber Position – Axial to radial/tangential curves can vary widely, by a factor of up to 10, depending on species. However, statistically, a lower percentage of Latewood result in a greater the resistance in the radial component and in a higher percentage it presents greater resistance in the tangential direction; (ii) Density – density variation, densification; (iii) Temperature – The effect of temperature is due to the variation of intermolecular forces of attraction (hydrogen bridges), which are weakened by the frequency of atomic or molecular oscillations caused by temperature. The magnitude of influence is additionally a function of the shape of the sample with which the characteristics are determined (-20°C to 60°C – 40%; -20°C to 150°C – 55% of the Modulus of Elasticity); (iv) Moisture – Wood should be understood as a partially porous, hygroscopic (absorbs moisture from the air) and capillary substance. The proportion of cavities on average is 50 to 60% of the volume. Wood can acquire and store water through capillary absorption and transport processes, better seen in Fig. 3.

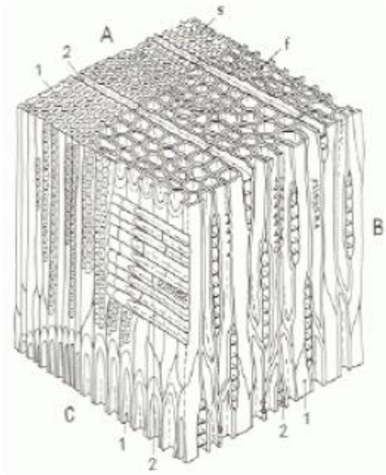

Figure 3: *Wood microstructure.*
Source: [1]

3. METHODOLOGY

The Oriented Strand Board (OSB) is a wood composite made from fine wood flakes primarily from commercially grown trees. The predominant orientation of the flakes gives it relatively higher mechanical properties in the direction of the flakes (the longitudinal direction of a board) than in the transverse direction. OSB is therefore an orthotropic material [5].

The results of the work carried out in [2] demonstrate that OSB is an orthotropic material with its strongest properties in the direction of wire orientation. OSB is stronger in compression. In traction, OSB behaves linearly to near failure, while in compression it exhibits plasticity. In elastic-plastic behavior in compression, it exhibits a stress-strain curve similar to a parabola. There is little difference in the OSB's modulus of elasticity in tension and compression, which allows a single value to be used in both cases. Thus, it was proposed through Benchmark 3 of [2], once the methodology and phenomena were validated through a solid model, to quantitatively predict the difference in the orientation of the flakes, or here also called fibers. The fibers were studied in two orientations, parallel and perpendicular to the compression.

Considering that the numerical simulations are performed with LS-DYNA [6], a computer code based on the finite element method, its material model 24 (MAT024 –

MAT_PIECEWISE_LINEAR PLASTICITY) is widely used in the simulation of shock-type events as an isotropic material model with the VON MISES stress flow criterion [7].

Benchmark 03, which is proposed by OAPIL [2], was modeled to represent the combination of a wooden cylinder encapsulated by a steel plate, resisting axial compression resulting from a free-fall impact of 9m. The goal is the assessment of the joint conformation of the two different materials and the performance of the interaction between them. Table 1 and Fig. 4 illustrates some geometric and materials information.

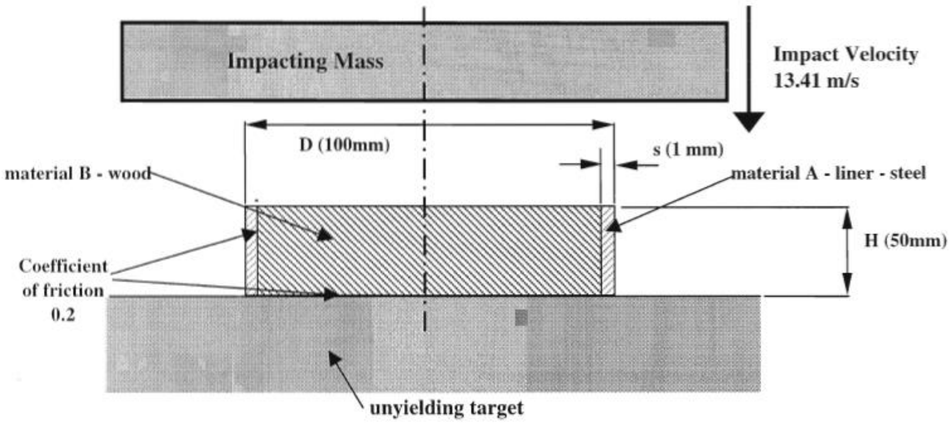

Figure 4: *Benchmark details.*
Source: [2]

In the study, all contacts are defined as friction and a friction coefficient set is 0.2 (Coulomb Coefficient), being Wood-Steel, Wood-Impactor, and Wood-Rigid Surface. To configure the 9m high free-fall motion, the final speed, or impact speed, was determined as 13.41m/s. Considering this speed, the period of observation of the behavior of the structure was estimated to be 5ms from the initial contact of the *Impactor* in wood. Impactor vertical displacement, Impact Force over time, and Maximum Wood Compression were defined as results of interest for analysis over time.

As mentioned before, the idea is to assess the wooden material as a shock absorber in a controlled situation, as mass impacting this encapsulated specimen with the characteristics described in the Figure 4.

Table 1: *Geometric and materials information. Source: [2], modified.*

Impacting Mass			**Material A - Liner**	**Mild steel**	
- Material type		Rigid	- Density	rho	7850 kg/m³
- Diameter	D	150 mm	- Young´s modulus	E	210 000 N/mm²
- Mass	M	100 kg	- Poisson´s ratio	nu	0.3
- Impact velocity	v	13.41 m/s	- Yield strength	SigY	200 N/mm²
			- Hardening modulus	Eh	1000 N/mm²
Wooden Impact Limiter			**Material B**	**Wood**	
- Overall Height	H	50 mm	- Material type	Perfectly Plastic	
- Overall Diameter	D	100 mm	- Density	rho	500 kg/m²
- Liner thickness	s	1 mm	- Yield strength	SigY	17 N/mm²
			- Hardening modulus	Eh	0 N/mm²

Two different approaches are proposed: the first and closest to the original study, in the 3D environment with two symmetry planes (1/4) with Liner modeled as shell elements; the second in a 2D axisymmetric environment that took two forms: one as a reproduction of the two previous cases (continuum mechanics) and another with the detailing of the fibers (wood/OSB) of the impact absorber (this one in two conditions, with fibers parallel and perpendicular to the loading).

However, recommended values of Poisson and Modulus of Elasticity, both necessary to characterize the material in the ANSYS Workbench LS-DYNA [4], were not identified in [2]. Therefore, in the different simulations presented, observing the due representation of a perfectly plastic behavior idealized for the wood, MAT024 was applied with the properties described in Table 1.

4. RESULTS AND DISCUSSION

These results are from different numerical modeling choices from the same case presented and described in Figure 4.

4.1. Liner modelled using shell elements

Considered as the control analysis, special attention was given to the contacts involved and mesh optimization studies were carried out, to represent with greater accuracy, the modelling of the original study. Mesh details can be observed in Fig. 5, as the element size in scale, the liner´s shell elements and the very small clearance between bodies to favor the convergence of non-linear contacts.

Figure 5: *Mesh details – control analysis.*
Source: Authors

The contacts, all with a friction coefficient of 0.2, were configured with an Offset close to 0.2mm and a Viscous Damping Coefficient of 10. It was not necessary to specify stiffness values. The default values of Soft Constraint Scale Factor (0.1) and Depth (1) were kept [6]. In Fig. 6, one may identify through the contacts Wood, Liner L and Liner S the respective force magnitude and the main reference from [2], when Liner L corresponds to the longitudinal stress and the liner S to the radial stress. This happen as the Liner itself is compressed its kinks.

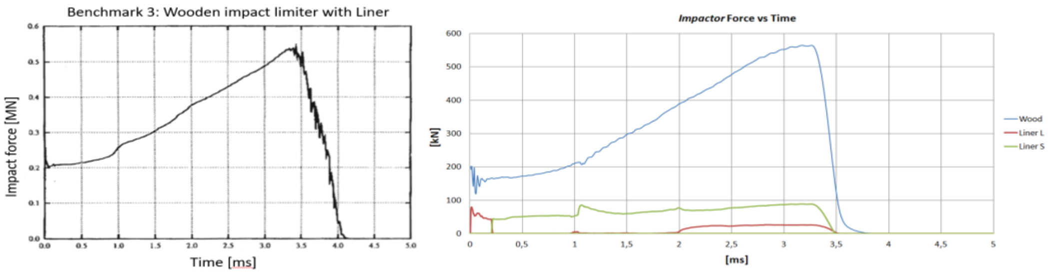

Figure 6: *Impact force vs time.*
Source: [2] and authors

After reproducing the behavior of the impact force overtime, the variation of this force was evaluated for the different combinations of v-E, respectively Poisson´s ratio and elastic modulus. The maximum displacements found showed no significant variation for the v-E variations (Fig. 7). The vertical displacement and the speed of the Impactor vs Time were evaluated as well (Fig. 8). The original study responses are on left and the present study responses, on right.

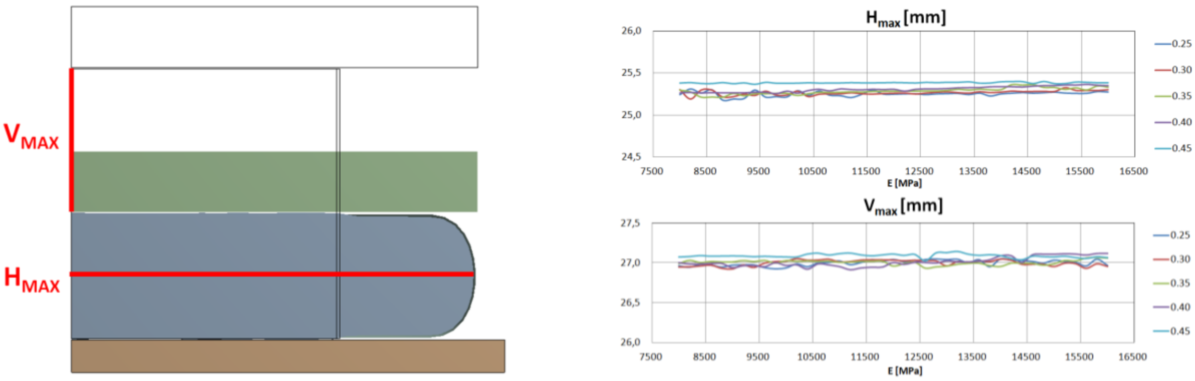

Figure 7: *Maximum displacement for different Poisson´s ratios and Youngs Modulus*
Source: Authors

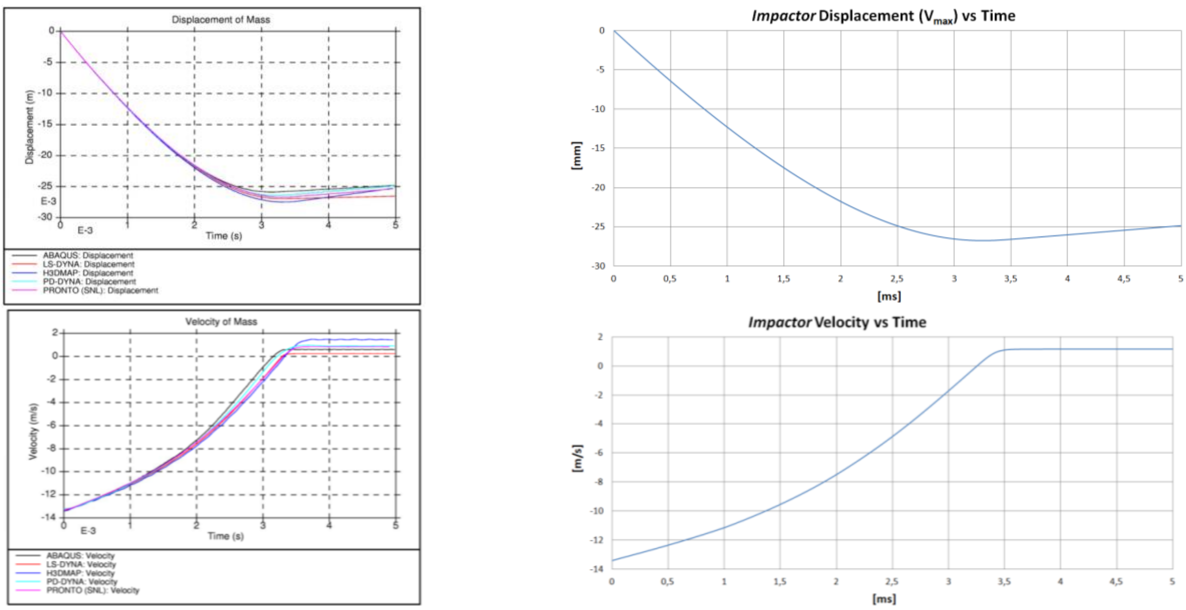

Figure 8: *Impactor displacement and speed vs time.*
Source: [8] (left) and authors (right)

In the impact force vs time graph, the forces exerted by the contacts modeled on the Impactor were presented, but it is also possible to extract the force acting on the rigid body through its acceleration in time. Applying the Result Tracker, with nodal selection, to any node of the body we can evaluate the behavior of the acting acceleration and correcting the mass for a 100 kg body since the calculation was run for two symmetries model, the relation between impactor force and time is reached in Fig. 9.

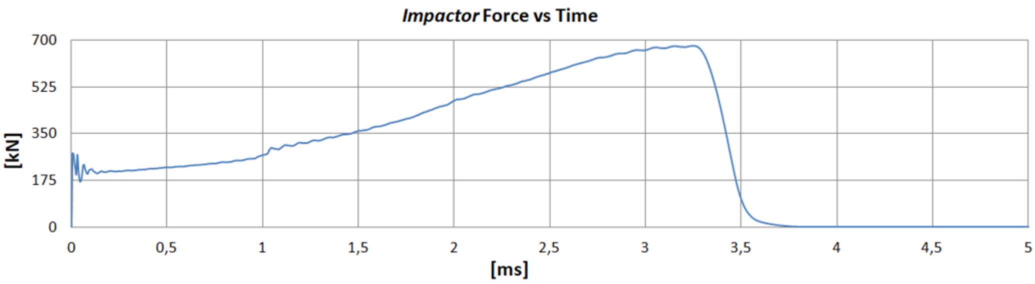

Figure 9: *Impactor force vs time.*
Source: Authors

Therefore, it is possible to identify the phenomenon presented with better correlation, without possible deviations in the behavior of the contacts. Thus, observing the combinations (v-E) previously defined, Figure 10 shows the small variation in Force (<1%), compared to the maximum value, when the Poisson and Modulus of Elasticity are varied.

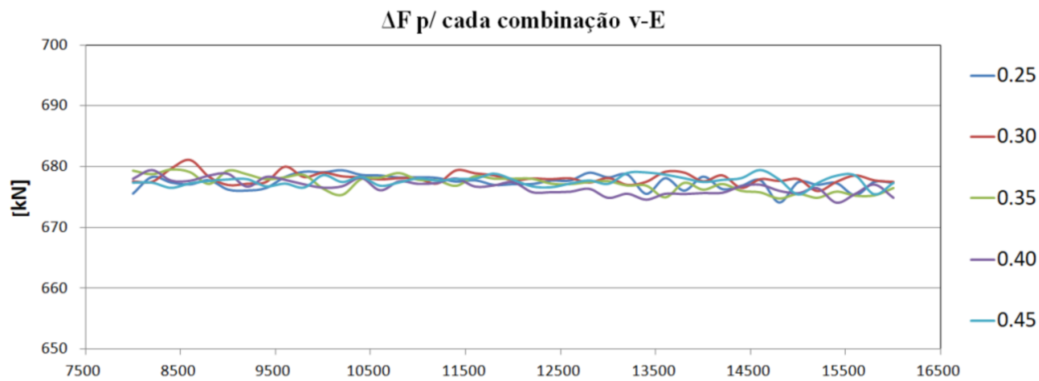

Figure 10: *Impactor force comparison.*
Source: Authors

4.2. Axisymmetric analysis

As suggested by the original study author [2], it is possible to perform this calculation in the 2D environment, considering axisymmetric behavior. In the present study, three types of modeling were explored: continuous medium; 1 mm fibers in two different orientations: only parallel to the load and only perpendicular. The required outputs were explored to confirm the Benchmark reproduction in a comparative way between the three different analyses. For the case without fibers, the contacts followed the definitions of the other analyses, for the cases in which the fibers were modeled, the coefficient of friction between them was considered to be 0.5. Fig. 11 illustrates the geometric and mathematics models, for the three analyses.

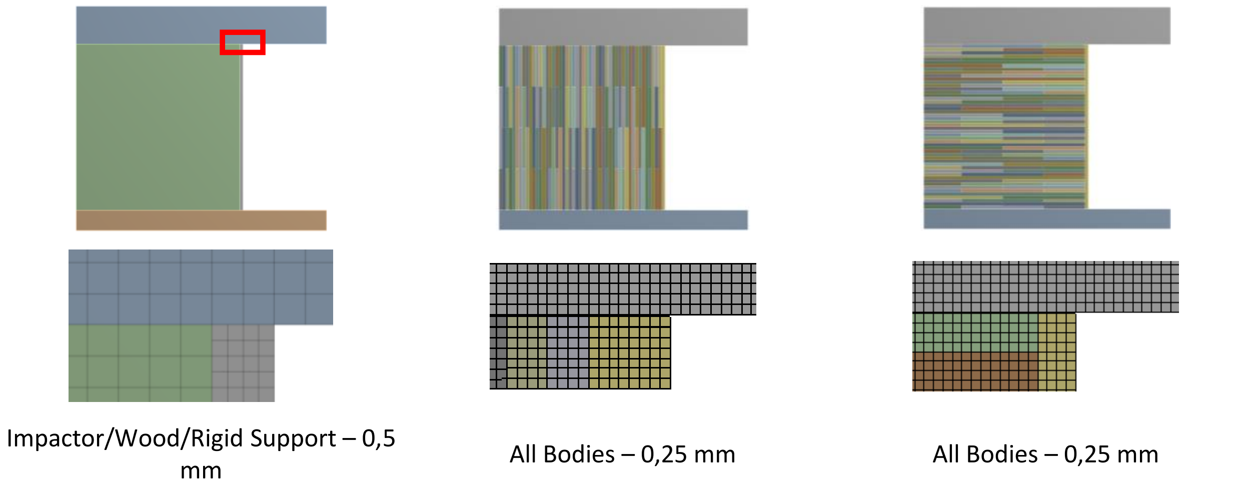

Figure 11: *Applied finite element models – (a) continuum; (b) parallel fibers; (c) perpendicular fibers;*
Source: Authors

4.2.1 No fibers case

The axisymmetric analysis was performed with the model presented in Figure 11(a). The v-E combination set in the analysis is in Table 2. The maximum horizontal and vertical displacements are shown in Fig. 12. Finally, Fig. 13 illustrates the variation of the impact force for each v-E set.

As shown below, the results of the analysis that does not consider fibers are overall in agreement with the results of section 3.1.

Table 2: v-E combination.

v	E	v	E	v	E	v	E	v	E
0,25	8000	0,3	8000	0,35	8000	0,4	8000	0,45	8000
0,25	9000	0,3	9000	0,35	9000	0,4	9000	0,45	9000
0,25	10000	0,3	10000	0,35	10000	0,4	10000	0,45	10000
0,25	11000	0,3	11000	0,35	11000	0,4	11000	0,45	11000
0,25	12000	0,3	12000	0,35	12000	0,4	12000	0,45	12000
0,25	13000	0,3	13000	0,35	13000	0,4	13000	0,45	13000
0,25	14000	0,3	14000	0,35	14000	0,4	14000	0,45	14000
0,25	15000	0,3	15000	0,35	15000	0,4	15000	0,45	15000
0,25	16000	0,3	16000	0,35	16000	0,4	16000	0,45	16000

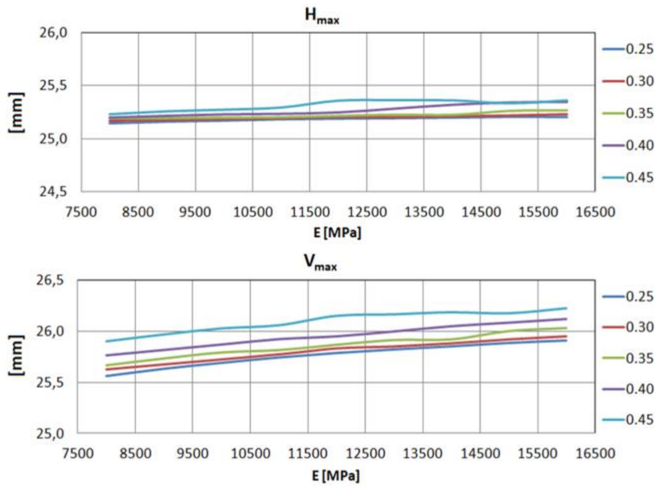

Figure 12: *Maximum displacements.*
Source: Authors

Figure 13: *Variation of the impact force.*
Source: Authors

4.2.2 Fibers consideration

The axisymmetric analysis was performed, as presented in Figure 11, using an isotropic material. The definition of friction at 50% between the fibers was used, imposing a behavior close to an orthotropic one, so the compression on fibers effect would be better simulated. Two orientations, perpendicular to the direction of compression and parallel to it, were modeled.

The v-E combination set in the analysis is in Table 3. The deformation line, for both fiber orientations, is observed in Figure 14. Finally, Figure 15 illustrates the variation of the impact force for each v-E set, for horizontal (left) and vertical (right) fiber orientation.

Table 3: v-E combination.

v	E	v	E	v	E	v	E	v	E
0,25	8000	0,3	8000	0,35	8000	0,4	8000	0,45	8000
0,25	10000	0,3	10000	0,35	10000	0,4	10000	0,45	10000
0,25	12000	0,3	12000	0,35	12000	0,4	12000	0,45	12000
0,25	14000	0,3	14000	0,35	14000	0,4	14000	0,45	14000

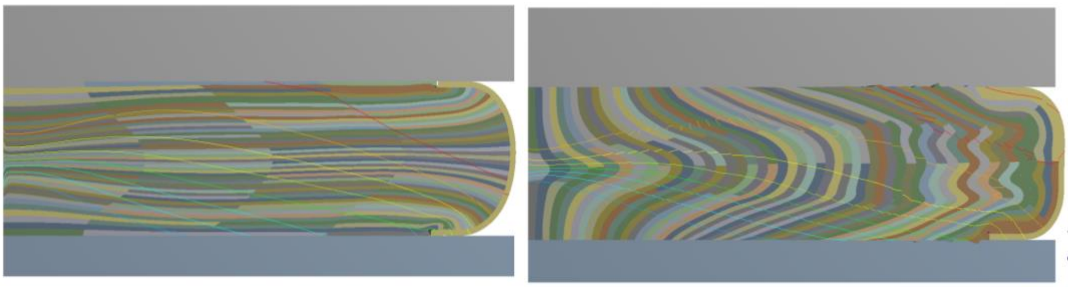

Figure 14: *Deformation line.*
Source: Authors

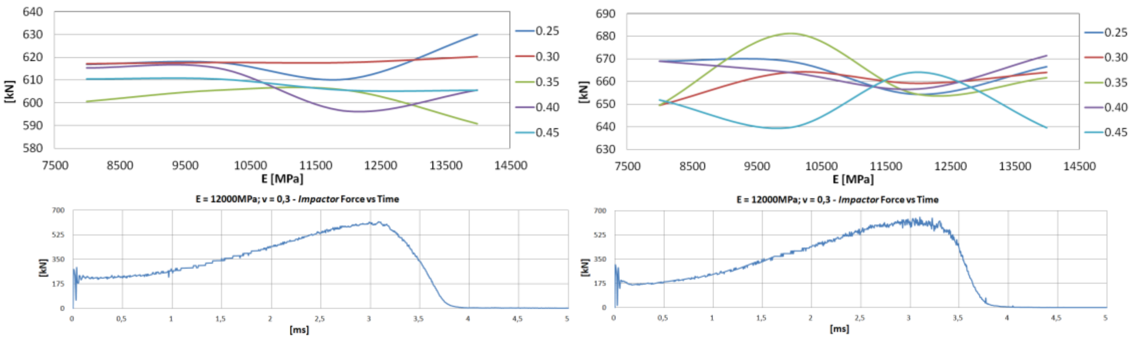

Figure 15: *Impact force for horizontal (left) and vertical (right) fiber orientation.*
Source: Authors

At this point, it was possible to comparatively notice the difference in the fiber deformation process and when the development of force in time in both cases was analyzed, it is possible to infer the influence of fiber kinking on the energy absorption potential.

Through this study, it is possible to comparatively notice the difference in the fiber deformation process and when observing the development of strength over time in both cases, one can infer the influence of the fiber's bending tendency on the energy absorption potential, increasing the absorption capacity by approximately 10% when compared between shock directions. One can evaluate the best design for its application for optimal protection.

5. CONCLUSION

In summary, it was possible to study advanced definitions of materials and reproduce the study developed in 1998 [2]. Objectively, through the analysis of session 3.1, it was demonstrated the application of material models where energy absorption is the main structural function. From the case of session 3.2, it was demonstrated that the orientation of the wood fiber became sensitive with an approximate difference of 10% more in the impact absorption potential, without considerable variation in the duration interval of the maximum deceleration. The next steps are: to explore bibliography on rigid polyurethane foams, apply this methodology and comparatively display the results. Once this step is completed, it is expected to apply in a satisfactorily calibrated model of numerical simulations of packaging for transporting research reactor spent fuel elements.

ACKNOWLEDGMENT

The authors are grateful to IPEN-CNEN for providing all the necessary means for the conclusion of this work.

REFERENCES

[1] NEUMANN, M. **Investigation of the Behavior of Shock-Absorving Structural Parts of Transport Casks Holding Radioactive Substances in Terms of Design Testing and Risk Analysis.** BAM-Dissertation Series, Volume 45, Berlin, Germany, 2009.

[2] Ove Arup and Partners International (OAPIL); Gesellschaft für Nuklear-Behälter mbH (GNB). **Evaluation of Codes for Analyzing the Drop Test Performance of Radioactive Material Transport Containers.** European Commission DG 17, United Kingdom, Germany, March 1998, Report Ref: 53276/02.

[3] GIBSON L.J.; ASHBY. M.F. **Cellular solids Structure and properties.** Cambridge University Press, London, England, 1997.

[4] NAIRN, J. A. **Numerical Modeling of Wood or Other Anisotropic, Heterogeneous and Irregular Materials.** 4th MPM Workshop, Salt Lake City, Utah United States of America, March, 2008.

[5] DING, Y.; Et al. **Dynamic crushing of cellular materials: A unique dynamic stress-strain state curve.** Mechanics of Materials vol. 100 (2016) pp. 219-231 September, 2016.

[6] LSTC - Livermore Software Technology Corporation**. LS-DYNA Keyword User's Manual R11.** Volume 1, Version 10580, 2018. Available at: <https://www.dynasupport.com/manuals/ls-dyna-manuals>. Last accessed: 10 Jul. 2020.

[7] LSTC - Livermore Software Technology Corporation. **LS-DYNA Keyword User's Manual R11.** Volume 2, Version 10572, 2018. Available at: <https://www.dynasupport.com/manuals/ls-dyna-manuals>. Last accessed: 10 Jul. 2020.

[8] CHI-FUNG TSO, Arup, UK e R. HÜGGENBERG. Evaluation of Finite Element Codes for Demonstrating the Performance of Radioactive Material Packages in Hypothetical Accident Drop Scenarios. **14th International Symposium on the Packaging and Transportation of Radioactive Materials** (PATRAM 2004), Berlin, Germany, September 20-24, 2004.